Available online at www.sciencedirect.com

ScienceDirect

Thermochimica Acta 466 (2007) 1–12

thermochimica acta

www.elsevier.com/locate/tca

Confined rapid thermolysis/FTIR/ToF studies of triazolium-based energetic ionic liquids

Arindrajit Chowdhury, Stefan T. Thynell*

Department of Mechanical and Nuclear Engineering, The Pennsylvania State University, University Park, PA 16802, USA

Received 2 August 2007; received in revised form 26 September 2007; accepted 27 September 2007
Available online 10 October 2007

Abstract

The thermal decomposition of two energetic ionic liquids, formed by pairing the 4-amino-1,2,4-triazolium cation with chloride (4ATCl), and nitrate (4ATN) anions, was studied by confined rapid thermolysis. Rapidscan FTIR spectroscopy and time-of-flight mass spectrometry were utilized in conjunction to identify the products of decomposition. Decomposition was achieved under heating rates of 2000 K/s and temperatures up to 340 °C for 4ATCl and 4ATN in an ambient inert gas at 1 atm. Whereas a proton transfer from the N_1 position primarily initiated decomposition in 4ATCl, the amino group was found to primarily participate in the initiation reaction in case of 4ATN. The parent molecule, 1-*H*-1,2,4-triazole, was detected during subsequent reactions. Ring fracture was also evident from the presence of HCN. The highly energetic nitrate salt formed copious amounts of H_2O and N_2O through multiple secondary reaction channels.

Keywords: Energetic ionic liquids; Thermal decomposition; FTIR spectroscopy; ToF mass spectrometry

1. Introduction

Ionic liquids are a unique class of salts with melting points below 100 °C, which have drawn recent attention due to their broad range of interesting properties [1–8]. The chemical and thermodynamic stability of these compounds, combined with their low vapor pressures and low melting points have put them forth as potential replacements of many noxious organic solvents used in the chemical industry [9,10]. Also their easy recoverability after usage has made them popular as "green solvents". However, interest has recently been drawn to heterocyclic ionic liquids with nitrogen-rich cations, such as imidazoles, triazoles and, tetrazoles, coupled with oxygen-rich anions such as nitrates, sulphates, and perchlorates, because of their high energy density. These compounds are easy to synthesize and their properties can be modified by alterations in their molecular structure.

Numerous synthesis, characterization and decomposition studies have been conducted on energetic salts containing the heterocyclic triazolium cation. Early, the focus was on the metalized salts involving the 5-nitro-2,4-dihydro-1,2,4-triazole-3-one (NTO) [11–16], and a complex between trinitromethane and 4-amino-1,2,4-triazole (4AT) [17]. Recently, significant strides in developing salts based on various derivatives of 1-*H*-1,2,4-triazole (1TA) or 1,2,3-triazole as cations and nitrates, perchlorates, and dinitramides as anions have been made by Shreeve and co-workers [18–25] and Drake et al. [26,27]. Since the hydrogen atoms on these azoles can be substituted easily by energetic functional groups, the family of the triazole salts has been expanded to include azido, amino, nitro, and nitramino azolium salts. The oxygen-rich substitute groups improve oxygen-balance of the cations and result in higher exothermicity during combustion. However, most of the thermal decomposition studies have been carried out using thermogravimetric analysis (TGA) and differential scanning calorimetry (DSC) under slow heating rates without any particular emphasis on the chemical kinetics of these decomposition reactions. Though these studies were carried out under low heating rates, the underlying trends provide valuable insights into the thermal stability of these compounds, the effects of various groups substituting the protons on the triazole ring, and their decomposition behavior under elevated heating rates. Some molecular modeling work has also been carried out to determine various macromolecular properties, such as melting point, heats of formation, etc. [28–33].

---

* Corresponding author. Tel.: +1 814 865 1345; fax: +1 814 865 6694.
E-mail address: Thynell@psu.edu (S.T. Thynell).

0040-6031/$ – see front matter © 2007 Elsevier B.V. All rights reserved.
doi:10.1016/j.tca.2007.09.009

Nitrate, perchlorate and dinitramide salts of 1,2,3-triazole, 1TA, and 4AT were prepared and characterized by Drake et al. [26]. Phase change and decomposition onset temperatures (T_d) were recorded using DSC, and mass-loss studies were also conducted by TGA. The dinitramide salts of all three cations were found to be the least stable, followed by the nitrates and the perchlorates. Shifting the ring nitrogen from the N_3 position to the N_4 position increased the T_d of 1,2,3-triazolium perchlorate from 200 to 285 °C, the probable reason being a decrease in the ease of ring-fracture through evolution of dinitrogen. Similar effects were observed with the nitrates and dinitramides. While the introduction of the amino group at the N_4 position lowered the thermal stability of the dinitramide salt, it increased the T_d of the perchlorate salt and had no effect on the nitrate salt. Nitrate, perchlorate and dinitramide salts of 3,4,5-triamino-1,2,4-triazole were also synthesized [27]. The order of thermal stability of these salts was found to be unaltered. Replacement of two ring H atoms with amino groups had no effect on T_d of the dinitramide salt, but the perchlorate and the nitrate salts showed an increased thermal stability. Theoretical calculations carried out to ascertain the geometry of the salts showed excellent agreement with X-ray diffraction studies.

Temperatures defining onset of thermal decomposition of a broad range of energetic ionic liquids have recently been established using thermogravimetric methods by Shreeve and co-workers [18–25]. Nitrate and perchlorate salts of amino and alkyl derivatives of 1TA were synthesized and their decomposition onset temperatures were recorded under a heating rate of 10 °C/min [21]. The results reiterate the increased stability of the perchlorate salts over the nitrate salts, as established by Drake et al. [26]. It is speculated that the hydrogen bonding between the amino group and the nitrate anion is reduced when the amino group is attached to N_4, as opposed to N_1. Though this causes a decrease in the melting point, T_d increased from 149 °C for 1-amino-1,2,4-triazolium nitrate to 181 °C for 4-amino-1,2,4-triazolium nitrate.

Novel energetic ionic liquids, with substituted 1,2,4-triazolium cations and azolate anions, such as 4,5-dinitroimidazolate and 5-nitrotetrazolate were prepared by Shreeve and co-workers [22]. The compounds with 5-nitrotetrazolate as the anion exhibited greater thermal stability and higher molar enthalpies of formation than the corresponding 4,5-dinitroimidazolate salts. 4-Amino-1,2,4-triazolium 4,5-dinitroimidazolate had the greatest T_d. Heats of formation showed an increased positive value due to the azido group on the ring.

Li and Litzinger [34] studied the thermal decomposition of 4ATN, driven by a CO_2 laser with a heat flux of 100 W/cm^2 in a helium environment at 1 atm. The gaseous products from the decomposition of the sample material in the condensed phase were analyzed by a triple quadrupole mass spectrometer. Though the temperatures of decomposition were not stated, under the extremely high heating rates applied, a proton transfer involving the N_1 position was identified as the initiation reaction. The resultant neutral species, HNO_3 and 4AT were found to react subsequently to produce mainly H_2O and N_2O through an ionic route analogous to the low-temperature decomposition of NH_4NO_3. The significant amount of 1TA detected among the products was attributed to the displacement of the amino group on 4AT by a hydrogen radical.

Schmidt et al. [29] employed ab initio quantum chemistry calculations of a gas-phase anion–cation pair to predict heats of formation and charge delocalization in energetic ionic liquids formed by the 1,2,4-triazolium cation family. Suitability of several groups, such as F, OH, NH_2, CH_3, CN, N_3, NF_2, NO_2, C_2H_3, and OCH_3 was tested as substituents on the 1,2,4-triazolium cation, while dinitramide was selected as the anion. Charge delocalization studies, integral to the prediction of lower melting points, suggested that only CN and the NF_2 groups degraded the resonance structures to a small extent, without hampering the ability of the cations to form ionic liquids. However, these two groups provide the maximum molar heats of formation, though CN is preferable, as N_3 involves forming a ring *exo* NN bond. Deprotonation studies with the parent cation and 4AT by geometry optimization indicate that deprotonation from the N_1 position is the possible first step during thermal decomposition. The factors responsible for deprotonation were small energy barriers and spontaneous proton-transfer from ionic dimers to form neutral pairs.

Several attempts have been made to predict melting points and other physical properties of the mono- or di-substituted 1,2,4-triazolium class of ionic liquids by molecular dynamics simulations or by quantitative structure-property relations (QSPRs). Factors affecting the melting points of ionic liquids include arrangements of atoms in the crystal lattice, interactions among ion-pairs, molecular symmetry, and conformational degrees of freedom. Alavi and Thompson [28] used molecular dynamics simulations, based on a force field modeled after the one developed by Lopes et al. [35] The method of void-induced melting predicted the melting point of 1-*n*-propyl-4-amino-1,2,4-triazolium bromide at 360 K, whereas the experimental melting point is 333 K. The velocity autocorrelation function indicated strong degrees of ion-counterion interactions common among systems with cage effects. Trohalaki et al. [30,31] derived QSPRs for melting points of 1-substituted-4-amino-1,2,4-triazolium bromide, nitrate, and nitrocyanamide salts from molecular orbital, electrostatic, and thermodynamic descriptors. The optimal molecular geometries of the cations were calculated using ab initio quantum chemical methods.

The goal of the current work is to identify the proton-transfer mechanism determining the initiation of decomposition of energetic aminotriazolium salts under isothermal conditions and high heating rates. Two synergistic diagnostic tools have been utilized for this purpose, Fourier transform infrared (FTIR) spectroscopy and time-of-flight (ToF) mass spectrometry (MS), leading to better probabilities of identifying the decomposition products and the reaction pathways. The salt of primary interest is 4-amino-1,2,4-triazolium nitrate (4ATN). Since the complexity of the secondary reactions is considerably higher for the oxygen-rich anion, the relatively simple salt 4-amino-1,2,4-triazolium chloride (4ATCl) has been studied initially. Extensive studies have also been conducted on the building blocks for these complicated molecules such as 4AT, 3-amino-1,2,4-triazole (3AT), and 1TA, as shown in Fig. 1.

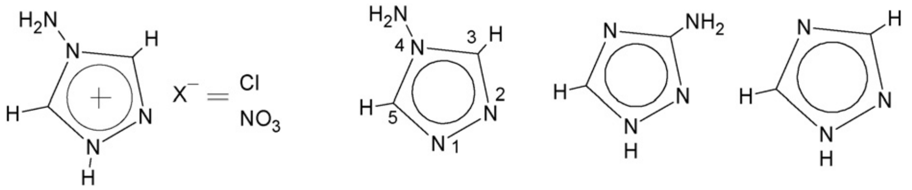

Fig. 1. Structures of 4-amino-1,2,4-triazolium X (X = chloride and nitrate), 4-amino-1,2,4-triazole, 3-amino-1,2,4-triazole, and 1-*H*-1,2,4-triazole.

2. Experimental approach

2.1. Experimental setup and diagnostic tools

Confined rapid thermolysis (CRT)/FTIR/ToF MS has been discussed in previous works [36,37]. The technique is very sensitive to decomposition processes occurring in the condensed phase, compared to the gas phase, as the molecules are quenched by the relatively cooler atmosphere into which they evolve. A brief summary of the technique is provided here. A small amount of the sample, approximately 0.5 mg, was confined between two heated, parallel surfaces within a constant pressure chamber. The surfaces belong to a stationary top heater and a mobile bottom heater, maintained at isothermal conditions by cartridge heaters controlled by PID controllers. After the thermolysis chamber is purged by an inert gas, the sample is rapidly heated to the set temperature at heating rates of 2000 K/s. The gaseous products evolving from the condensed phase are sampled by a modulated FTIR beam passing through two ZnSe windows. Thus the spectra are obtained in near real-time with a spectral resolution of 2 cm^{-1} and a temporal resolution of 50 ms. As the two heaters came in contact, one notes a slight base-line shift in the spectral transmittance that serves as the indicator for the beginning of heating. The products are also sampled by a ToF MS system (Model D-677 from R.M. Jordan, www.rmjordan.com), equipped with a 1 m flight tube and a 44 mm microchannel plate (MCP) detector. In this system, molecular beam sampling is done by directing the evolved gases towards a 100 μm orifice, which separates the 1st stage of the ToF mass spectrometer from the thermolysis chamber.

2.2. Data reduction in FTIR spectroscopy

A non-linear, least-squares method is utilized to extract the species concentrations of the evolved gases by comparison with theoretical transmittance [38]. The radiative properties, such as partition function, half-width of spectral lines, and its temperature exponent, are determined from the HITRAN database [39]. The measured gas-phase temperature serves as an input to the data-reduction technique. The computational procedure involves specifying the total pressure, measured gas-temperature profile, and assumed path length. The algorithm computes the partial pressures, and coefficients for linear base-line shifts. Iterations are continued until a change in the sum of the errors between successive guesses is less than 0.01%. After completion of the iterations, the relative concentrations of various species, such as H_2O, N_2O, NO_2, NO, CO, CO_2, HCl, NH_3 and HNO_3 are obtained for each spectrum.

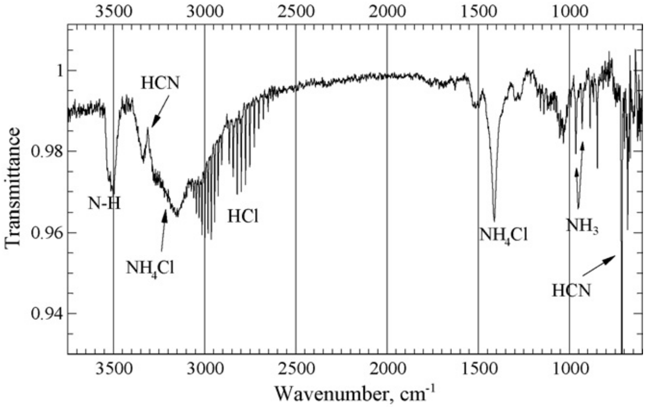

Fig. 2. FTIR spectrum of species from rapid thermolysis of 4ATCl at 340 °C and 1 atm N_2.

3. Results and discussion

3.1. Thermal decomposition pathways of 4ATCl

4ATCl was procured from Sigma–Aldrich and subjected to confined rapid thermolysis without further purification. The salt is a white crystalline solid with a melting point of 147–148 °C. Approximately 0.5 mg of the sample was found to rapidly decompose above temperatures of 260 °C, leaving a small amount of solid yellowish residue on the aluminum foil.

The gaseous products from the decomposition of 4ATCl under 340 °C and an inert atmosphere of N_2 are shown in Fig. 2. The products identified in the FTIR spectrum are HCl, HCN, NH_3, and NH_4Cl. The vibrational frequencies of the experimentally observed species are listed in Table 1.

Around 3500 cm^{-1}, a strong N–H absorption band was observed. In order to identify the source of the band, 4AT (99% pure), 3AT (95% pure), and 1TA (98% pure) were acquired from Sigma–Aldrich and studied under temperatures around 340 °C. All the three compounds are crystalline white solids.

Table 1
Vibrational frequencies of experimentally observed gaseous products

Description	Frequency (cm^{-1})
H_2O	3657 (s), 1595 (s)
HCN	3311 (s), 2097 (w), 712 (vs)
NH_3	3336 (m), 1626 (s), 968 (vs), 933 (vs)
CO_2	3716 (w), 3609 (w), 2326 (vs), 741 (m), 667 (vs)
N_2O	2457 (vs), 2217 (vs), 1302 (vs), 1275 (vs)
HNO_3	3550 (m), 1709 (vs), 1326 (s), 1304 (vs), 879 (s)

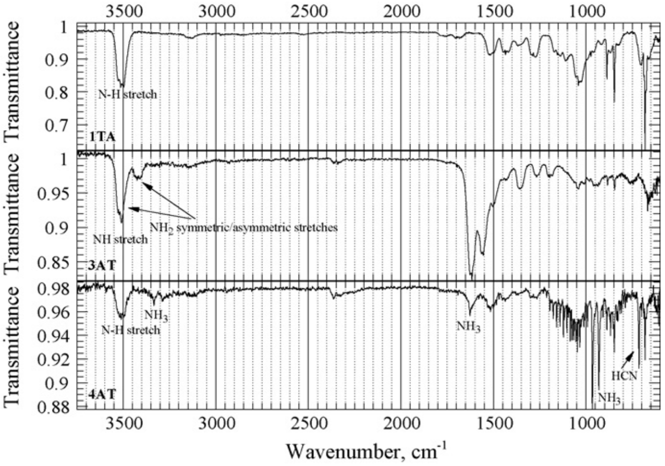

Fig. 3. Comparison of FTIR spectra of 4AT, 3AT and 1TA.

Table 2
Comparison of rovibrational frequencies of 1TA with standard data [40]

Description	Frequency (cm^{-1}) (predicted)	Frequency band (cm^{-1}) (experimental)
=C–H str	3157/3149	3175–3100
C–N str, C–H def	1524	1540–1480
C–N str, C–H def	1407	1475–1400
C–N str	1265/1255	1300–1240
C–N str, C–H def	1175	1190–1160
N–N str	1042	1075–1000
C–H wag	826	900–800
Ring torsion	710/706	740–650

Fig. 3 shows a comparison of the transmission spectra from the thermolysis of the three compounds. The difference between 3AT and 1TA is evident in the region around 3500 cm^{-1}, where two bands due to a symmetric and an asymmetric stretch in the –NH_2 group distinguishes 3AT. Similar stretches due to the presence of the –NH_2 group are clearly visible in gas-phase transmission spectra from aniline. Though the =C–H stretching frequency is observed for both of these heterocyclic compounds around 3125 cm^{-1}, dissimilarities exist between 1650 and 600 cm^{-1}. The C–N stretches at 1625 and 1550 cm^{-1}, present in the gas-phase FTIR spectrum of 3AT is absent in case of 1TA.

Whereas 3AT and 1TA were found to evaporate without decomposition, 4AT decomposed significantly to yield NH_3, HCN and a heterocyclic compound. To assist in the identification of species evolving during the decomposition of 4AT, Fig. 4 shows the results from the thermolysis of 4AT under an inert atmosphere of Ar and He, acquired under an ionization potential of 70 eV and mass spectra acquisition at 1000 Hz. Averaging 10 consecutive spectra were found to provide a high degree of accuracy with the standard deviation of the intensities staying below a value of 5 units. Besides the compounds detected by FTIR spectroscopy, N_2 was produced in profuse quantities. The heterocyclic compound mentioned earlier was found to have a molecular weight of 69, and was established as 1TA. The IR-active vibrational modes of the triazole molecule have been documented by El-Azhary et al. [33] and are summarized in Table 2. The predicted C–N stretches at 1524, 1407, 1255, and 1175 cm^{-1} were recognizable in the spectrum. The C–H deformation or bending-in-plane frequencies were identified too.

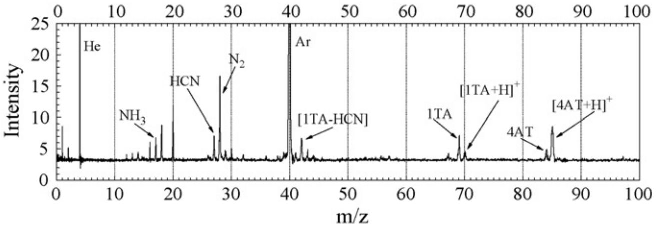

Fig. 4. Mass spectrum from rapid thermolysis of 4AT.

Decomposition of 4AT was initiated by the N_4–N bond scission, leading to the formation of the amino radical and 4*H*-1,2,4-triazol-4-yl, as proposed by the reaction Pathway I. 4*H*-1,2,4-Triazole is formed by a hydrogen transfer to 4*H*-1,2,4-triazol-4-yl from the amino radical or from another 4AT molecule. 4*H*-1,2,4-Triazole undergoes tautomerization to form the thermodynamically more stable, 1TA, as suggested by Palmer and Christen [40]. Similar tautomeric forms were detected by flash vacuum thermolysis of 1TA by Wentrup and Flammang [41], leading to N_2 elimination from the least stable tautomer, 3*H*-1,2,4-triazole.

An electron transfer to the N_1 atom from the N_4 atom converts 4*H*-1,2,4-triazol-4-yl to 1*H*-1,2,4-triazol-1-yl, which subsequently participates in proton-abstraction to form 1TA. The amino and the imino radicals also initialize a radical-driven chain reaction, portrayed in Pathway II, leading to the formation of NH_3 and N_2 in the process, with intermediates such as diimide and dinitrogen monohydride.

In order to clearly identify the products of decomposition of 4ATCl in the region 1500–600 cm^{-1}, spectra from 4ATCl, 4AT, 1TA, and NH_4Cl are compared in Fig. 5. 99.9% NH_4Cl from

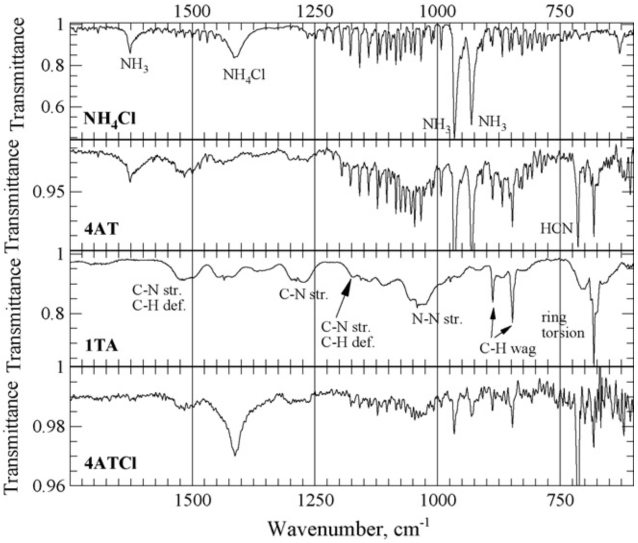

Fig. 5. FTIR spectra of NH_4Cl, 4AT, 1TA, and 4ATCl for identification of thermolysis products.

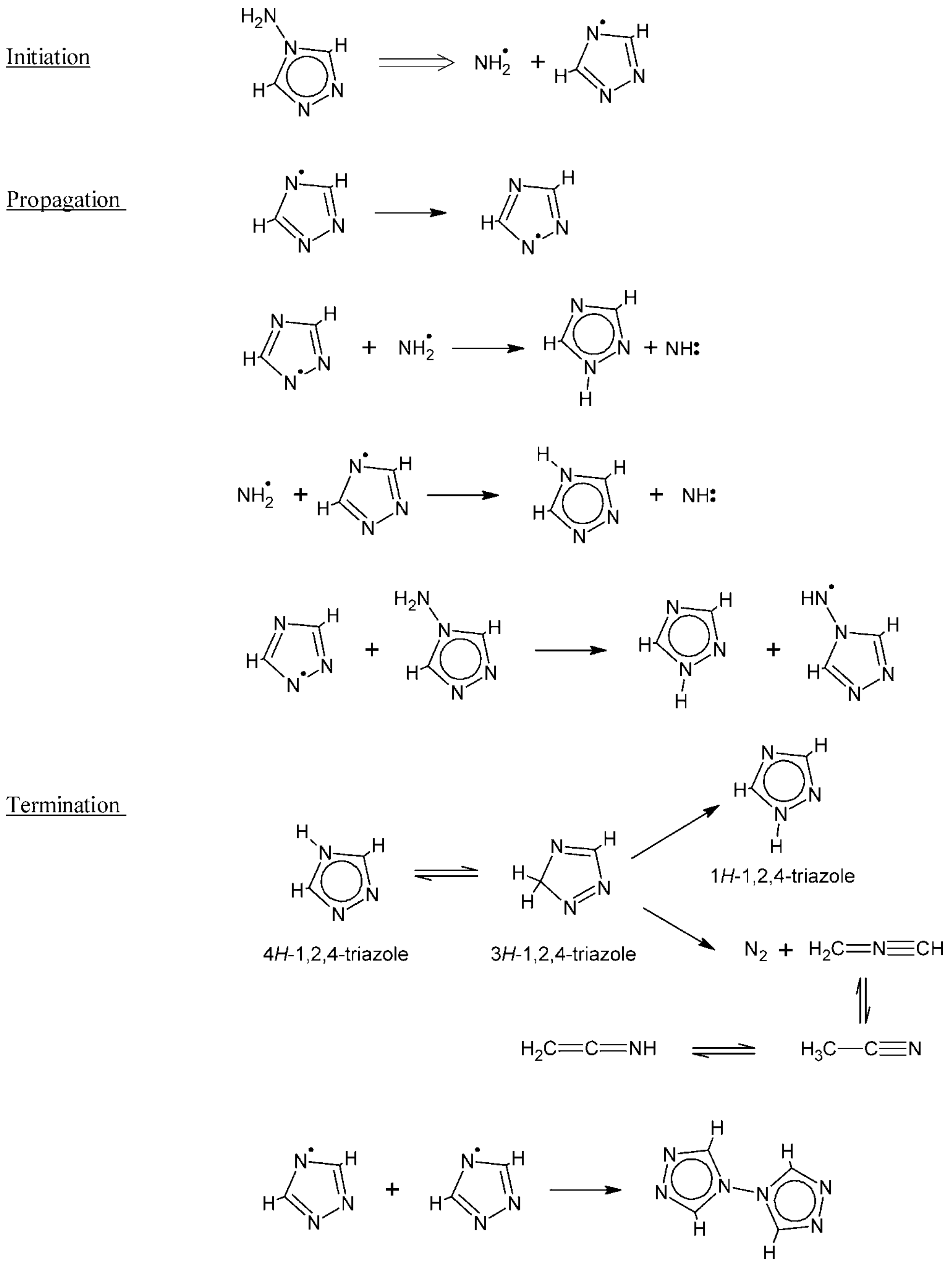

Pathway I. Proposed major steps in the decomposition of 4AT to form 1TA.

Sigma–Aldrich was heated to 525 °C in order to obtain its gas-phase spectrum. NH_3, HCN, and NH_4Cl are clearly discernable in the spectrum from 4ATCl.

The presence of the NH_3 rotational lines from 1200 to 750 cm^{-1} proved to be a hindrance in clearly identifying the vibrational bands from 1TA in that region. However, the N–N stretch at 1042 cm^{-1} and the C–H wagging frequencies were recognized easily. Also visible was the ring torsion frequency at 710/706 cm^{-1}. The source of NH_3, present among the decomposition products of 4ATCl, could be attributed to either 4AT or NH_4Cl. In order to resolve this ambiguity and to explain the thermolysis of 4ATCl, the products were further analyzed by ToF mass spectrometry.

Fig. 6 shows the results from the thermolysis of 4ATCl at 335 °C and an inert atmosphere of Ar and He. The various species are found to evolve at a fast rate and then decay immediately as the small amount of the sample is exhausted. A cursory glance at the spectra shows an abundance of HCl at $m/z = 35$, 36, 37, and 38. Also present are 1TA ($m/z = 69$) and HCN ($m/z = 27$). The signal at $m/z = 70$ was formed by the excess protonation of 1TA, due to the presence of H^+ ions in the flight tube of the ToF MS. The presence of atmospheric nitrogen, a species that is IR-inactive, obscured the evolution of N_2 during the actual decomposition of 4ATCl. The signals observed at $m/z = 41$, 42, and 43 were formed primarily by fragmentation of the ring due to the high ionization potentials used. Detailed discussion of

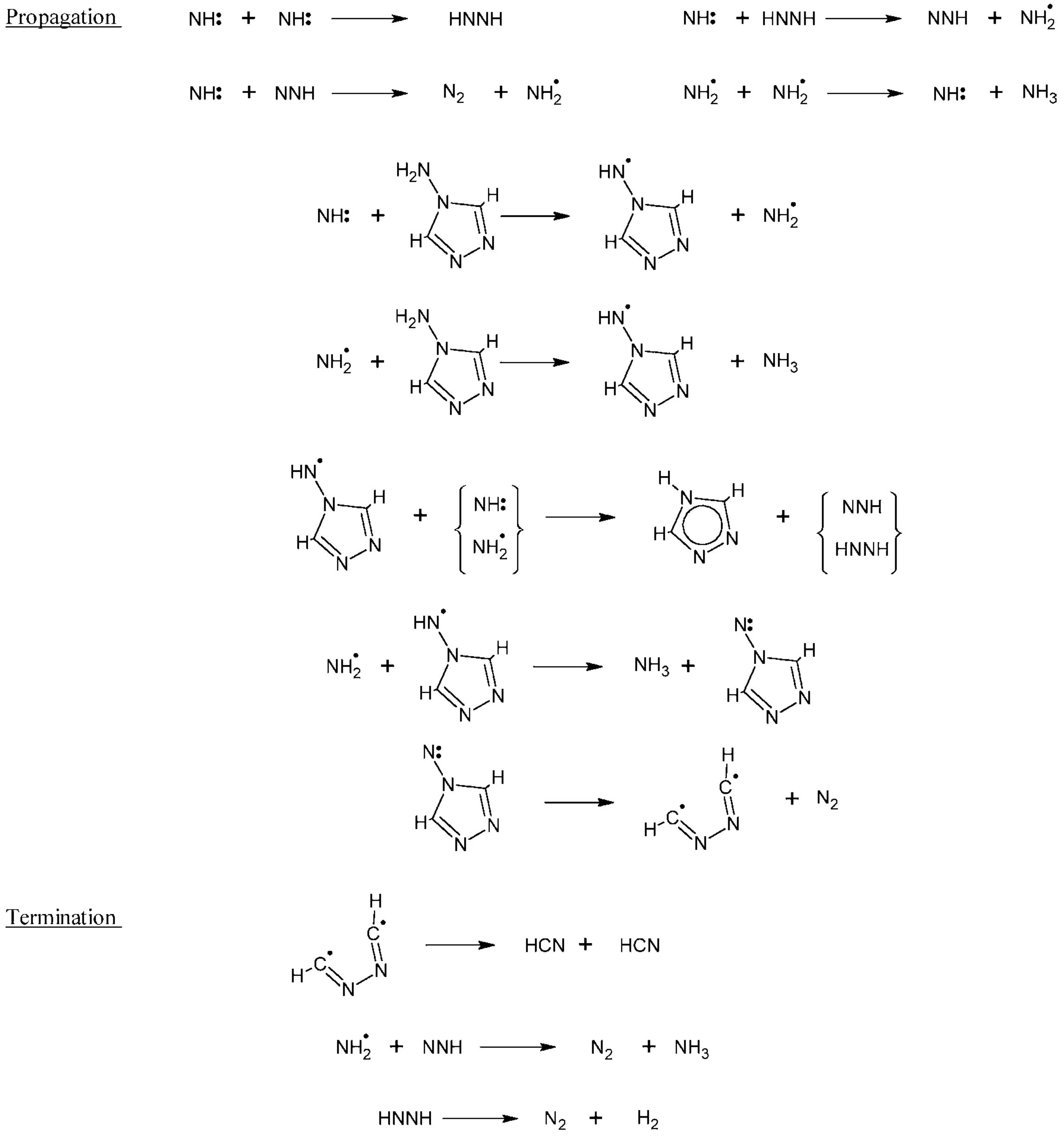

Pathway II. Proposed steps in the decomposition of 4AT to form NH3 and HCN.

the fragmentation pathways can be found in similar works [42]. However, no signal was detected at *m*/*z* = 84 (4AT).

In order to elucidate the decomposition pathways of 4ATCl, the species evolution profiles were extracted from the FTIR spectra and displayed in Fig. 7. Since quantification of some of the evolved species, such as NH_4Cl, would be difficult owing to their tendency to condense out in the gas phase during measurement, the evolution of these species has been studied just qualitatively. After a fairly short induction period of about 400 ms, HCl starts to desorb from the condensed phase at a very high rate, followed by HCN, 1TA, and NH_4Cl, after a significant delay. NH_3 appears considerably later than HCl and at a relatively slower rate.

The presence of copious amounts of HCl very early in the event and relatively smaller amounts of HCN and 1TA indicate a hydrogen-transfer from the N_1 atom (Pathway III), forming 4AT in the process. Though it remained undetected by the ToF MS, 4AT decomposes in the condensed phase under the applied temperatures, forming HCN, 1TA, NH_3, and N_2 according to Pathways I and II. NH_3, thus formed, recombines with HCl to form the detected NH_4Cl. A second, but minor reaction pathway (Pathway IV) involves the N_4–N bond cleavage to form HCl, an imino radical and 1TA, or NH_2Cl, an extremely reactive species, which then proceeds to abstract hydrogen from 4ATCl or 1TA to form $NH_4Cl{\cdot}NH_2Cl$ was not detected in the gas phase due to its reactive nature. The imino radical undergoes a series of reactions to form ammonia. However, this pathway is less important, due to the lack of a suitable pathway leading to the formation of HCN·1TA, a byproduct of the initial step of pathway IV, and the most likely source of HCN, is a fairly stable molecule, and would remain intact despite the proton-scavenging capabilities of the imino and amino radicals.

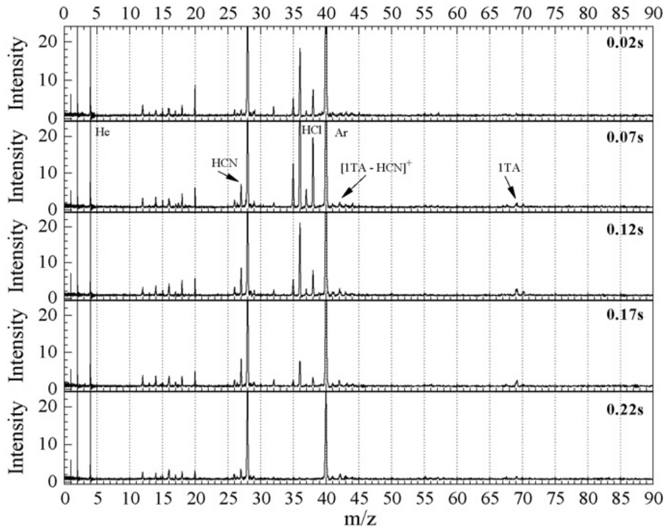

Fig. 6. Mass spectra from rapid thermolysis of 4ATCl at 340 °C and 1 atm Ar, He and residual air extracted at 0.02, 0.07, 0.12, 0.17, and 0.22 s (average of 10 spectra).

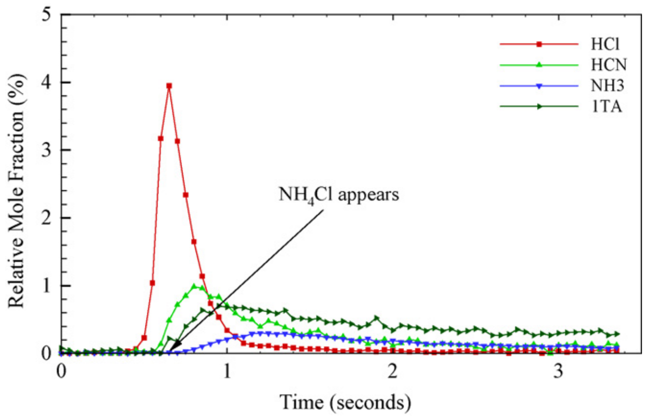

Fig. 7. Species evolution from rapid thermolysis of 4ATCl at 340 °C and 1 atm N_2.

3.2. Thermal decomposition pathways of 4ATN

4ATN, which is a white crystalline solid under standard conditions, has a melting point of 69 °C. Rapid thermolysis of the compound was found to occur at temperatures above 260 °C. Below that temperature, the sample remained on the foil without any discoloration. Fig. 8 shows the various species from thermolysis of 4ATN at 340 °C and a pressure of 1 atm of N_2. The various products identified in the spectrum were HNO_3, with three strong bands from 1700 to 900 cm^{-1}, and an overtone above 3500 cm^{-1}, N_2O, CO_2, and H_2O. Also evident are the N–H stretching frequency at 3500 cm^{-1}, the =C–H stretch around 3125 cm^{-1}. The presence of trace amounts of CO_2 was attributed to impurities in the sample and subsequent reactions with HNO_3. In the spectral range from 1500 to 600 cm^{-1}, assignment was aided by calibration compounds 4AT and 1TA. Fig. 9 shows the typical spectral transmittances of 4AT, 1TA, NH_3, and the gaseous products from 4ATN in the ‘fingerprint region’. From prior discussions, it was clear that the decomposition products of 4ATN contained the stable compound 1TA. Fig. 10 substantiates the presence of HNO_3, and indicates the absence of NH_4NO_3 among the decomposition products of 4ATN. The HNO_3 spectrum was obtained from the HITRAN database [39], whereas NH_4NO_3 was subjected to thermolysis at 340 °C.

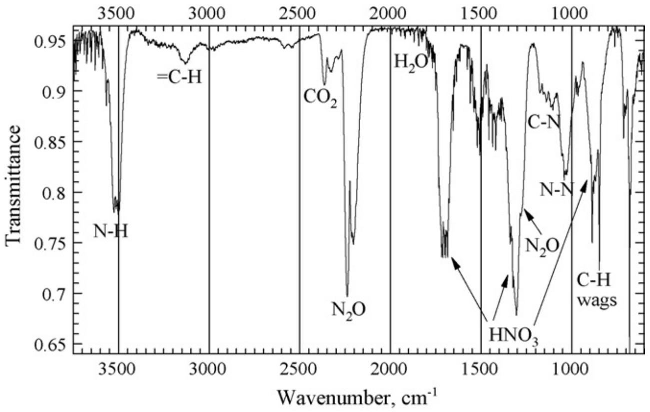

Fig. 8. FTIR spectrum of species from rapid thermolysis of 4ATN at 340 °C and 1 atm N_2.

The findings obtained from FTIR analysis were confirmed by ToF mass spectra. Fig. 11 shows the evolution of species from the thermolysis of 4ATN at 335 °C and 1 atm of argon and helium. The high ionization potential of 70 eV introduces certain levels of ambiguity in the spectra. The slight disadvantage

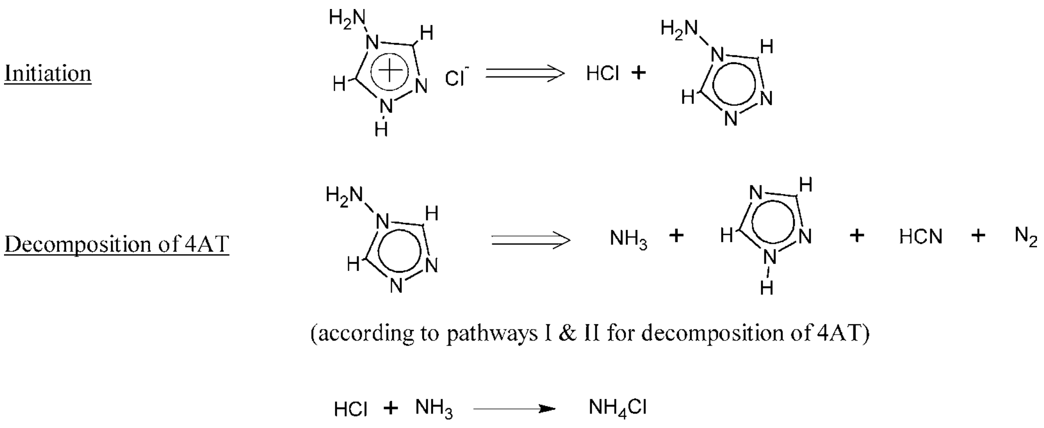

Pathway III. Proposed primary reaction pathway for 4ATCl.

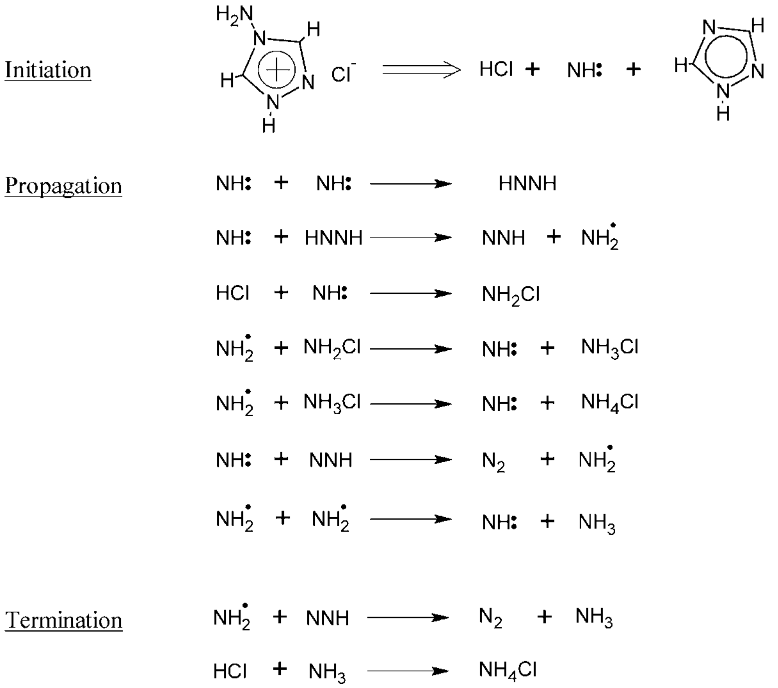

Pathway IV. Proposed secondary reaction pathway for 4ATCl.

is overshadowed by the ability to compare data with available mass spectral databases. At a first glance, the copious amounts of HNO_3 detected from the FTIR spectra seem to be absent due to the lack of a strong peak at $m/z = 63$. However, previous studies [43] showed that HNO_3 readily decomposes under the high ionization potential used to form NO_2^+ ($m/z = 46$), NO^+ ($m/z = 30$), H^+ ($m/z = 1$) and a number of other smaller ions, which were present in the mass spectra acquired during the early stages of the event.

The absence of a strong peak at $m/z = 84$ corroborates the absence of appreciable amounts of 4AT among the decomposition products. The larger peak at $m/z = 70$ was believed to be

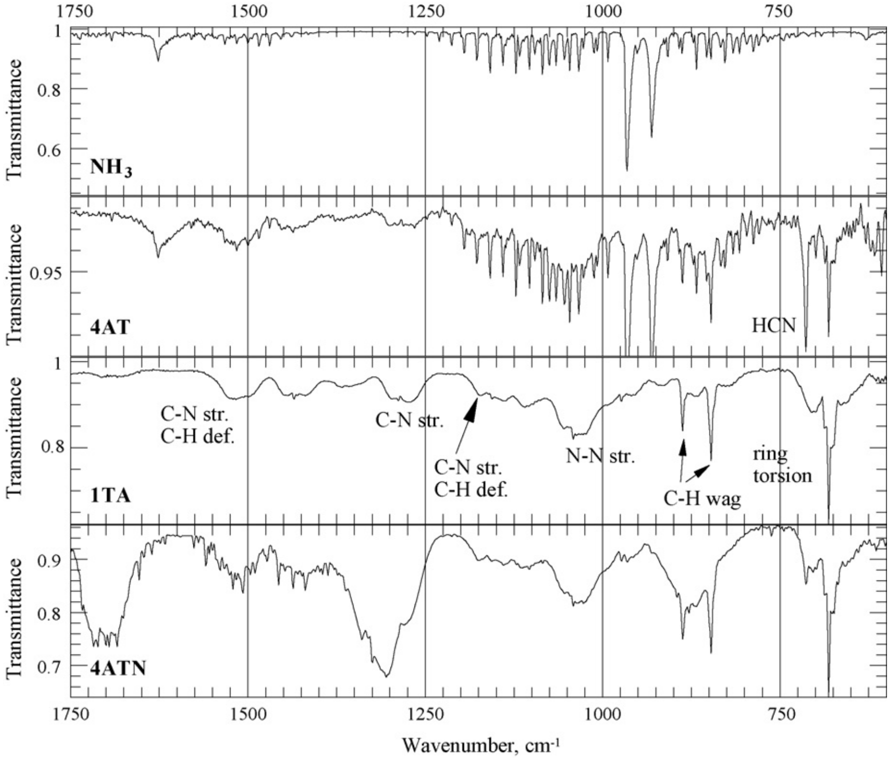

Fig. 9. FTIR spectra of NH_3, 4AT, 1TA, and 4ATN at 340 °C and 1 atm of N_2 for identification of thermolysis products.

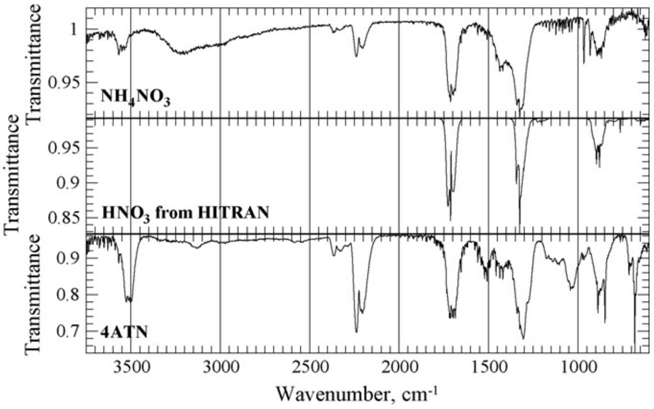

Fig. 10. FTIR spectra of NH_4NO_3, HNO_3, and 4ATN at 340 °C and 1 atm of N_2 for identification of thermolysis products.

caused by excess protonation of 1TA ($m/z = 69$) due to the presence of H^+ ions derived from fragmentation of HNO_3. Tests conducted at lower pressures essentially eliminated the peak at $m/z = 70$. The peak at $m/z = 44$ is attributed to N_2O, also present in the FTIR spectra. Occurrence of peaks at $m/z = 41$, 42 and, 43 was primarily due to the fragmentation of the ring.

A study of the species evolution profiles, extracted from the FTIR spectra, reveals further information on the decomposition pathways of 4ATN. Fig. 12 presents the profiles at 320 °C. Similar to 4ATCl, HNO_3 was found to evolve at an extremely fast rate after a short induction period. The presence of the strongly oxidizing nitrate anion led to the formation of H_2O and N_2O, both of which evolved at a slower rate than HNO_3. Compared to 4ATCl, the major difference in the species profiles was the early evolution of 1TA, and the relatively low concentrations of

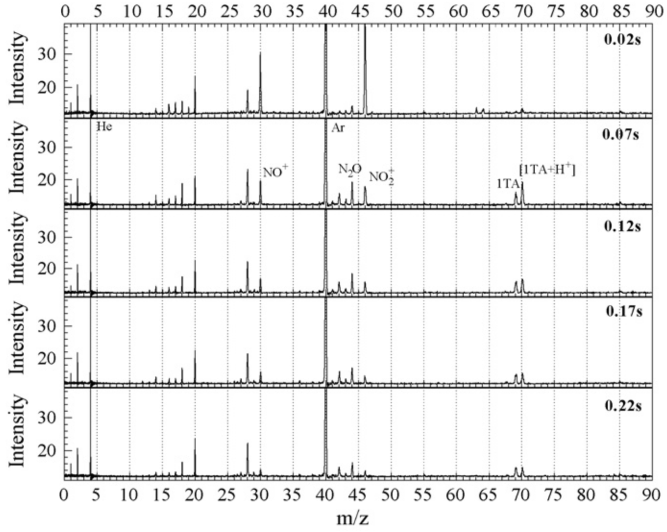

Fig. 11. Mass spectra from rapid thermolysis of 4ATN at 335 °C and 1 atm Ar, He and residual air extracted at 0.02, 0.07, 0.12, 0.17, and 0.22 s (average of 10 spectra).

HCN in the gas phase, implying an N_4–N bond scission as the primary initiation step.

The desorption of 1TA into the gas phase very early during the decomposition suggests that the transfer of a ring hydrogen to form HNO_3 is not a major pathway. Instead, the nitrate ion scavenges a proton from the amino group to form the large amounts of HNO_3 and 1TA, as shown by Pathway V. Although the generated HNO_3 escapes partially from the condensed phase, the remaining portion either establishes a partial equilibrium to generate the oxidizing species NO_2^+, according to Rosser et al. [44], or undergoes a homolytic fission to form the OH

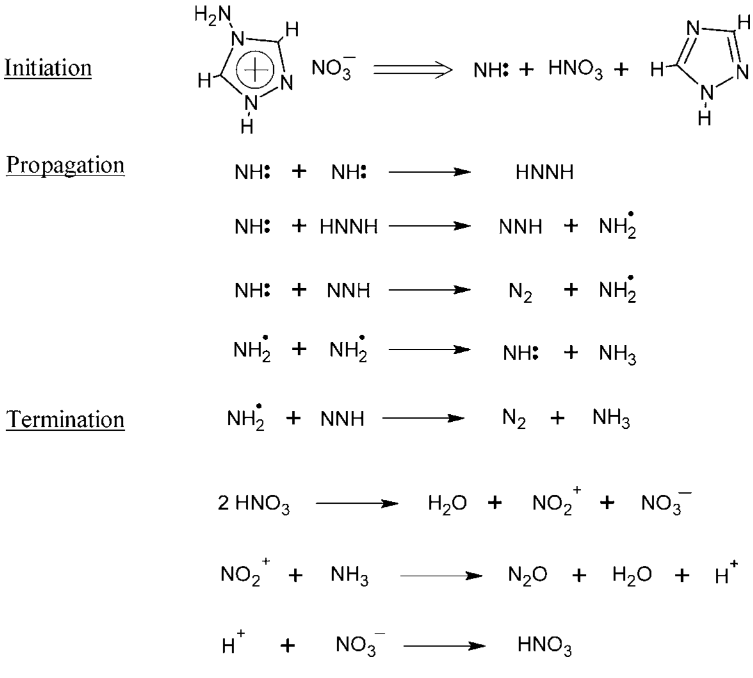

Pathway V. Proposed primary reaction pathway for 4ATN (ionic route).

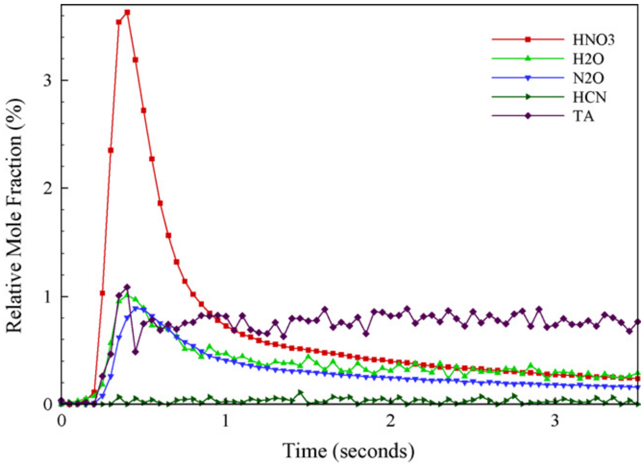

Fig. 12. Species evolution from rapid thermolysis of 4ATN at 320 °C and 1 atm N_2.

radical, followed by the evolution of gaseous nitrogen dioxide, as suggested by Brower et al. [45] and shown in Pathway VI.

The imino radical formed during the initiation step forms NH_3, following Pathway II for decomposition of 4AT, which is subsequently oxidized to N_2O and H_2O, by the oxidizing species generated from HNO_3. However, Pathway V is granted precedence over Pathway VI, due to the lack of NO_2 among the gaseous species detected by the FTIR spectrometer. Also, deamination and successive formation of H_2O and N_2O was found to be a major reaction pathway during deamination of 4-aminotriazolium salts using nitrous acid [46]. According to Pathway VII, the formation of the reactive species NH_2NO_3 is also a possibility, which promptly decomposes to form HNO and HNO_2.

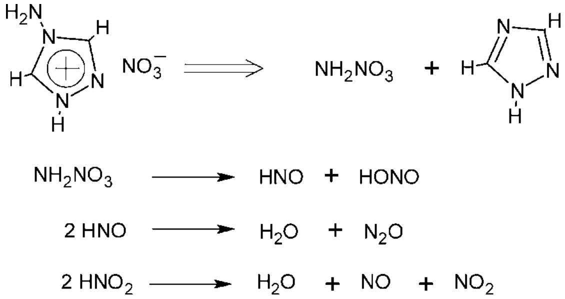

Pathway VII. Proposed alternate reaction pathway for 4ATN.

The variation of the initial reaction pathway due to presence of the nitrate anion needs to be clarified further. There are two probable reasons behind the formation of the protonated acids by deprotonation form two separate sites. The first of them being, the significant difference of the pK_a values of HCl and HNO_3. Since HCl is a stronger acid than HNO_3, this leads to a larger basicity of the conjugate base, the nitrate anion over the chloride anion. Studies by Brill and Ramanathan [47] involving hydrohalide salts of the energetic molecule 5-amino-1*H*-tetrazole illustrated the precedence of a radically different pathway of decomposition as the basicity of the halide anion was altered. Thus, similar trends can be expected in case of 4-amino-1*H*-triazolium salts.

The second reason involves the molecular structure of 4ATN and 4ATCl in the condensed phase. According to crystal structures determined by Laus et al. [32], on an average, the chloride anion resides closer to the N_1=H, compared to the NH_2 group,

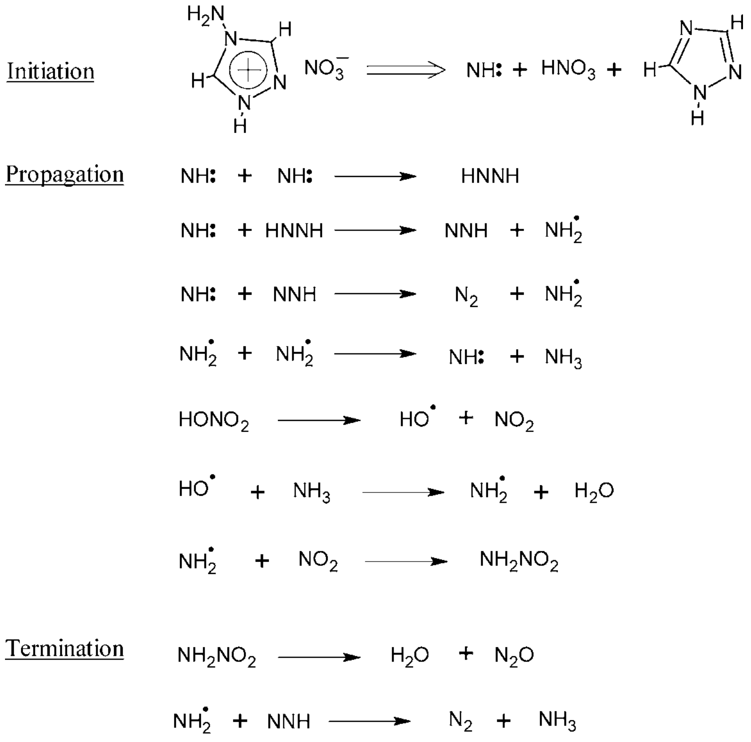

Pathway VI. Proposed primary reaction pathway for 4ATN (radical-driven route).

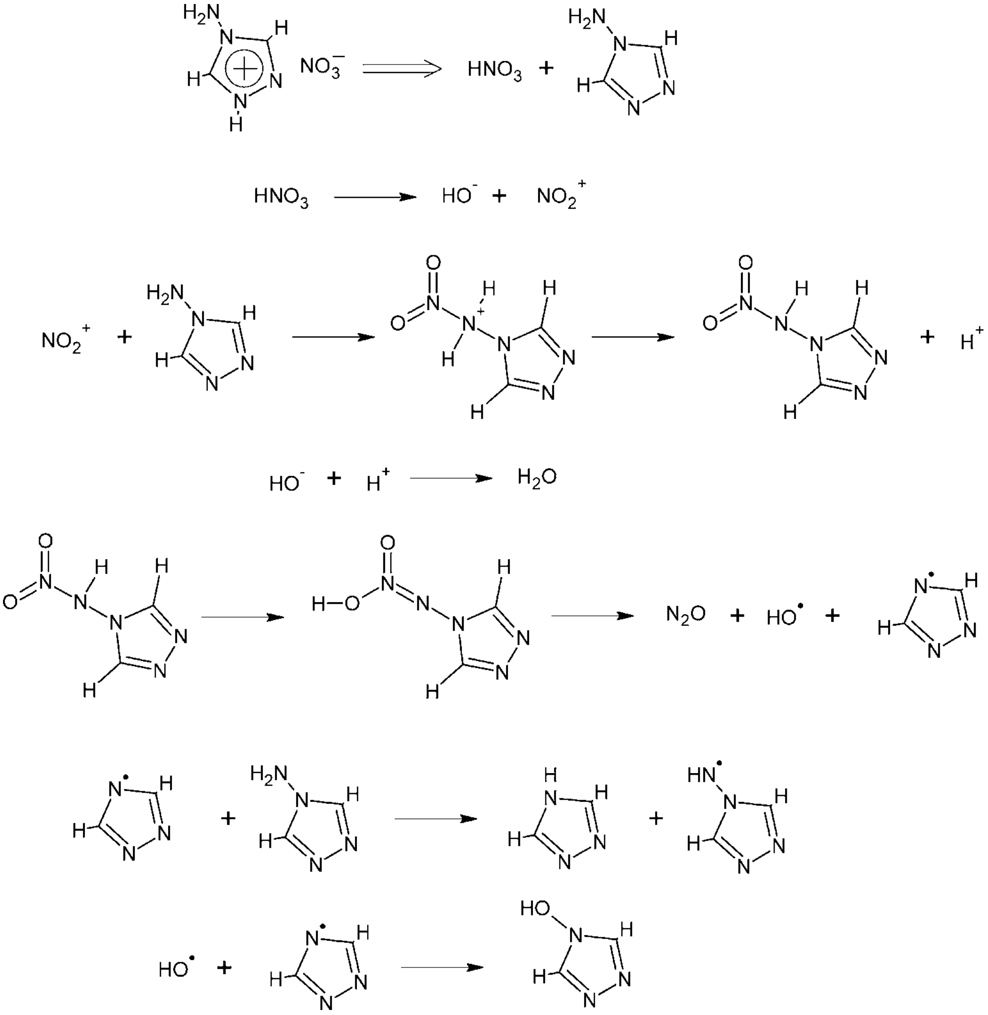

Pathway VIII. Proposed secondary reaction pathway for 4ATN.

thus increasing the probability of the formation of HCl by abstraction of the ring hydrogen during thermolysis. However, recent simulations by Cadena and Maginn [48] speculate that in case of 4ATN, the amino group is more readily accessible by the anion, as opposed to the ring hydrogens, thus providing a channel for the formation of HNO_3 via cleavage of the N_4–N bond. Similar discrepancies in initiation pathways based on different anions have been noted by Fischer et al. [49] while investigating thermal decomposition characteristics of 1,5-diamino-4-methyl-1-*H*-tetrazolium nitrate, dinitramide and azide. While decomposition was initiated by a proton transfer in case of the dinitramide and the azide salts to form the corresponding acids, a methyl group transfer was observed to be the initial process in case of the nitrate salt.

The secondary reaction pathway, as depicted by Pathway VIII, involves deprotonation at the N_1 position, to form nitric acid, and 4AT. Nitric acid produces the nitronium ion in the condensed phase, which produces N_2O and H_2O through deamination of 4AT. The 4*H*-1,2,4-triazol-4-yl radical, generated as a byproduct, abstracts a hydrogen atom from surrounding species to form the unstable 4*H*-1,2,4-triazole, which undergoes tautomerism to form 1*H*-1,2,4-triazole. The lack of HCN, a significant product of the decomposition of 4AT, in the gas-phase spectra of 4ATN leads to the conclusion that the proposed pathway is indeed secondary.

4. Conclusions

Confined rapid thermolysis studies with FTIR spectroscopy and ToF mass spectrometry as the diagnostic tools were conducted on two triazolium-based compounds, 4ATCl, and 4ATN. Deprotonation from the amino group initiated the decomposition for the more energetic 4ATN, with subsequent reactions leading to the formation of 1TA. No evidence of formation of 4AT was found, thus reducing the possibility of a proton transfer from the N_1 position. Multiple secondary reactions involving ring fracture were also apparent, leading to the formation of HCN. The species formed during the initial decomposition of 4ATN were extremely reactive, and produced smaller molecular weight species, such as H_2O and N_2O, at a fast rate.

Acknowledgments

This material is based upon work supported by the U.S. Air Force Office of Scientific Research under Contract No. FA9550-07-1-0432, with Dr. Michael Berman serving as the program manager. Funding for the purchase of the time-of-flight mass spectrometer by the U.S. Army Research Office under Contract No. DAAD19-01-1-0449, with Dr. David M. Mann serving as the program manager, is gratefully acknowledged. Sincere thanks go to Drs. Hawkins and Drake of Edwards AFB for providing 4ATN.

References

[1] A.A. Fannin, D.A. Floreani, L.A. King, J.S. Landers, B.J. Piersma, D.J. Stech, R.L. Vaughn, J.S. Wilkes, J.L. Williams, J. Phys. Chem. 88 (1984) 2614–2627.

[2] J.S. Wilkes, M.J. Zaworotko, J. Chem. Soc., Chem. Commun. 13 (1992) 965–967.

[3] J.D. Holbrey, K.R. Seddon, Clean Products Processes 1 (4) (1999) 223–236.

[4] A.S. Larsen, J.D. Holbrey, F.S. Tham, C.A. Reed, J. Am. Chem. Soc. 122 (2000) 7265–7272.

[5] J.S. Wilkes, J.A. Levisky, R.A. Wilson, C.L. Hussey, Inorg. Chem. 21 (3) (1982) 1263–1264.

[6] J. Sun, M. Forsyth, D.R. MacFarlane, J. Phys. Chem. B 102 (44) (1998) 8858–8864.

[7] P. Bônhote, A.-P. Dias, N. Papageorgiou, K. Kalyanasundaram, M. Grätzel, Inorg. Chem. 35 (5) (1996) 1168–1178.

[8] J. Shah, J. Brennecke, E. Maginn, Green Chem. 4 (2002) 112–118.

[9] M.J. Earle, K.R. Seddon, Pure Appl. Chem. 72 (7) (2000) 1391–1398.

[10] T. Welton, Chem. Rev. 99 (1999) 2071–2083.

[11] T.R. Botcher, D.J. Beardall, C.A. Wight, L. Fan, T.J. Burkey, J. Phys. Chem. 100 (1996) 8802–8806.

[12] N.L. Garland, H.D. Ladouceur, H.H. Nelson, J. Phys. Chem. A 101 (1997) 8508–8512.

[13] G.T. Long, B.A. Brems, C.A. Wight, J. Phys. Chem. B 106 (2002) 4022–4026.

[14] D.F. McMillen, D.C. Erlich, C. He, C.H. Becker, D.A. Shockey, Combust. Flame 111 (1997) 133–160.

[15] E.F. Rothgery, D.E. Audette, R.C. Wedlich, D.A. Csejka, Thermochim. Acta 185 (1991) 235–243.

[16] T.B. Brill, T.L. Zhang, B.C. Tappan, Combust. Flame 121 (2000) 662–670.

[17] V.I. Slovetskii, V.M. Brusnikina, L.I. Khmel'nitskii, O.V. Lebedev, Khim. Geterotsikl. Soedin. 2 (1966) 448.

[18] Y. Gao, S.W. Arritt, B. Twamley, J.M. Shreeve, Inorg. Chem. 44 (2005) 1704–1712.

[19] H. Xue, J.M. Shreeve, Adv. Mater. 17 (2005) 2142–2146.

[20] Y.R. Mirzaei, H. Xue, J.M. Shreeve, Inorg. Chem. 43 (2004) 361–367.

[21] H. Xue, S.W. Arritt, B. Twamley, J.M. Shreeve, Inorg. Chem. 43 (2004) 7972–7977.

[22] H. Xue, Y. Gao, B. Twamley, J.M. Shreeve, Inorg. Chem. 44 (2005) 5068–5072.

[23] H. Xue, Y. Gao, B. Twamley, J.M. Shreeve, Chem. Mater. 17 (2005) 191–198.

[24] H. Xue, B. Twamley, J.M. Shreeve, J. Org. Chem. 69 (2004) 1397–1400.

[25] H. Xue, B. Twamley, J.M. Shreeve, Inorg. Chem. 44 (2005) 7009–7013.

[26] G. Drake, T. Hawkins, A. Brand, L. Hall, M. Mckay, A. Vij, I. Ismail, Propellants, Explos., Pyrotech. 28 (2003) 174–180.

[27] G.W. Drake, T.W. Hawkins, J. Boatz, L. Hall, A. Vij, Propellants, Explos., Pyrotech. 30 (2005) 156–163.

[28] S. Alavi, D.L. Thompson, J. Phys. Chem. B 109 (2005) 18127–18134.

[29] M.W. Schmidt, M.S. Gordon, J.A. Boatz, J. Phys. Chem. A 109 (2005) 7285–7295.

[30] S. Trohalaki, R. Pachter, QSAR Comb. Sci. 24 (2005) 485–490.

[31] S. Trohalaki, R. Pachter, G.W. Drake, T. Hawkins, Energy Fuels 19 (2005) 279–284.

[32] G. Laus, V. Kahlenberg, D.M. Tobbens, R.K.R. Jetti, U.J. Griesser, J. Schutz, E. Kristeva, K. Wurst, H. Schottenberger, Cryst. Growth Des. 6 (2006) 404–410.

[33] A.A. El-Azhary, H.U. Suter, J. Kubelka, J. Phys. Chem. A 102 (1998) 620–629.

[34] J. Li, T.A. Litzinger, Thermochim. Acta 454 (2007) 116–127.

[35] J.N. Canongia Lopes, J. Deschamps, A.A.H. Padua, J. Phys. Chem. B 108 (2004) 2038–2047.

[36] E.S. Kim, H.S. Lee, C.F. Mallery, S.T. Thynell, Combust. Flame 110 (1997) 239–255.

[37] A. Chowdhury, S.T. Thynell, Thermochim. Acta 443 (2006) 164–177.

[38] C.F. Mallery, S.T. Thynell, Combust. Sci. Technol. 122 (1997) 113–129.

[39] L.S. Rothman, D. Jacquemart, A. Barbe, D. Chris Benner, M. Birk, L.R. Brown, M.R. Carleer, C. Chackerian Jr., K. Chance, L.H. Coudert, V. Dana, V.M. Devi, J.-M. Flaud, R.R. Gamache, A. Goldman, J.-M. Hartmann, K.W. Jucks, A.G. Maki, J.-Y. Mandin, S.T. Massie, J. Orphal, A. Perrin, C.P. Rinsland, M.A.H. Smith, J. Tennyson, R.N. Tolchenov, R.A. Toth, J. Vander Auwera, P. Varanasi, G. Wagner, J. Quant. Spectrosc. Radiat. Transfer 96 (2005) 139–204.

[40] M.H. Palmer, D. Christen, J. Mol. Struct. 705 (2004) 177–187.

[41] C. Wentrup, R. Flammang, J. Phys. Org. Chem. 11 (1998) 350–355.

[42] M. Ohashi, N. Ohno, H. Kakisawa, Org. Mass Spectrom. 1 (1968) 703–712; J.V. Thuijl, K.J. Klebe, J.J.V. Houte, Org. Mass Spectrom. 7 (1973) 1165–1172.

[43] C.S.S. O'Connor, N.C. Jones, S.D. Price, Int. J. Mass Spectrom. Ion Proc. 163 (1997) 131–139.

[44] W.A. Rosser, S. Inami, H. Wise, J. Phys. Chem. 67 (1963) 1753.

[45] K.R. Brower, J.C. Oxley, M. Tewari, J. Phys. Chem. 93 (1989) 4029–4033.

[46] B.A. Astleford, G.L. Joe, J.G. Keay, E.F.V. Scriven, J. Org. Chem. 54 (1989) 731–732;
M.D. Rosa, P. Haberfield, J. Org. Chem. 46 (1981) 2639–2643.

[47] T.B. Brill, H. Ramanathan, Combust. Flame 122 (2000) 165–171.

[48] C. Cadena, E.J. Maginn, J. Phys. Chem. 110 (2006) 18026–18039.

[49] G. Fischer, G. Holl, T.M. Klapotke, J.J. Weigand, Thermochim. Acta 437 (2005) 168–178.